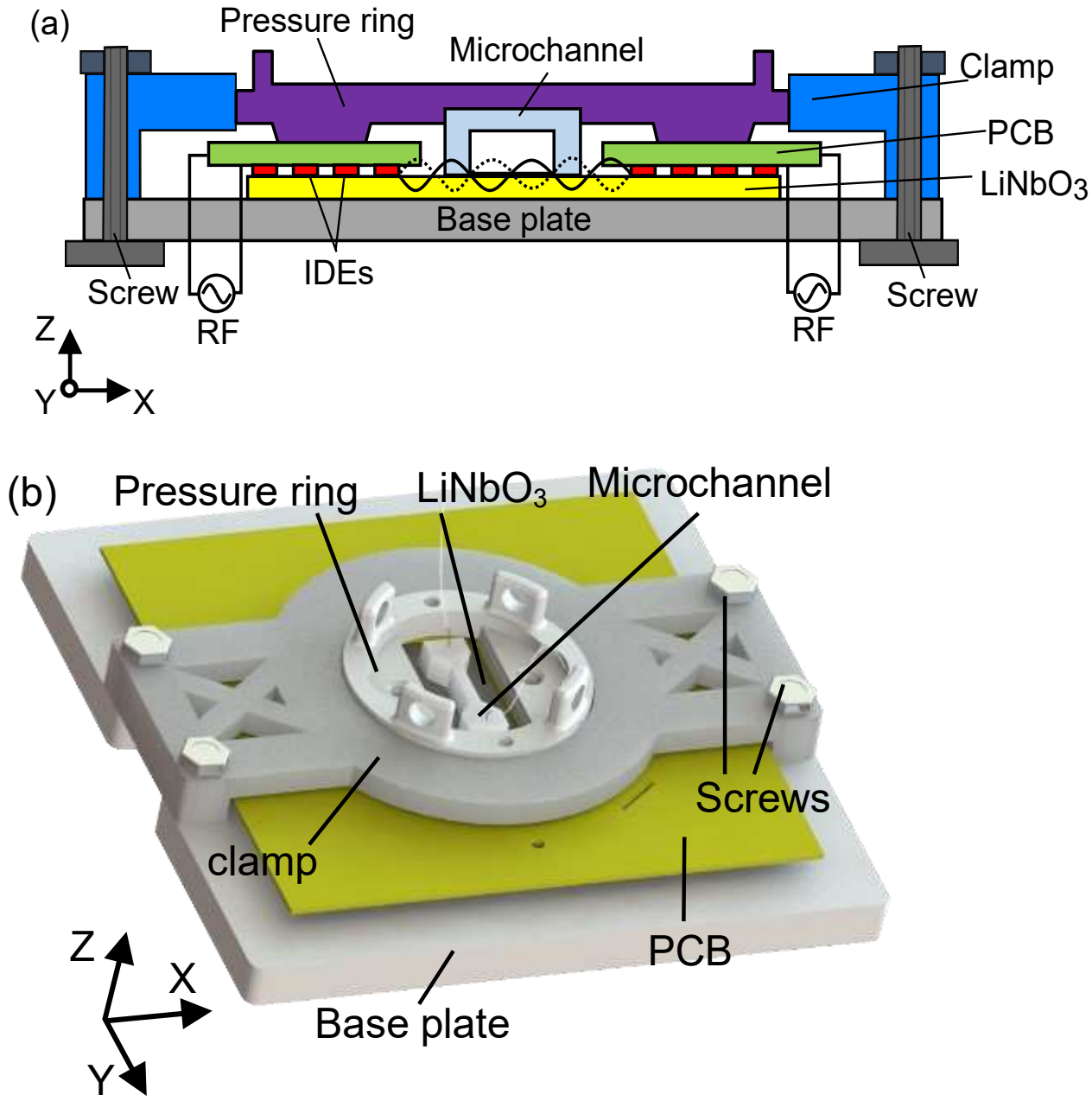

Figure 1. Schematic of the PCB-based surface acoustic wave (PCB-SAW) device. (a) Cross-sectional view of the PCB-SAW structure, consisting of a base plate, a clamp, a pressure ring, a PCB patterned with IDEs, a $LiNbO_3$ wafer and a microchannel. The PCB and the $LiNbO_3$ wafer are clamped by the mechanical jig to produce proximity for radio frequency signals coupling onto the wafer to produce SAW. (b) 3D model of the PCB-SAW device.

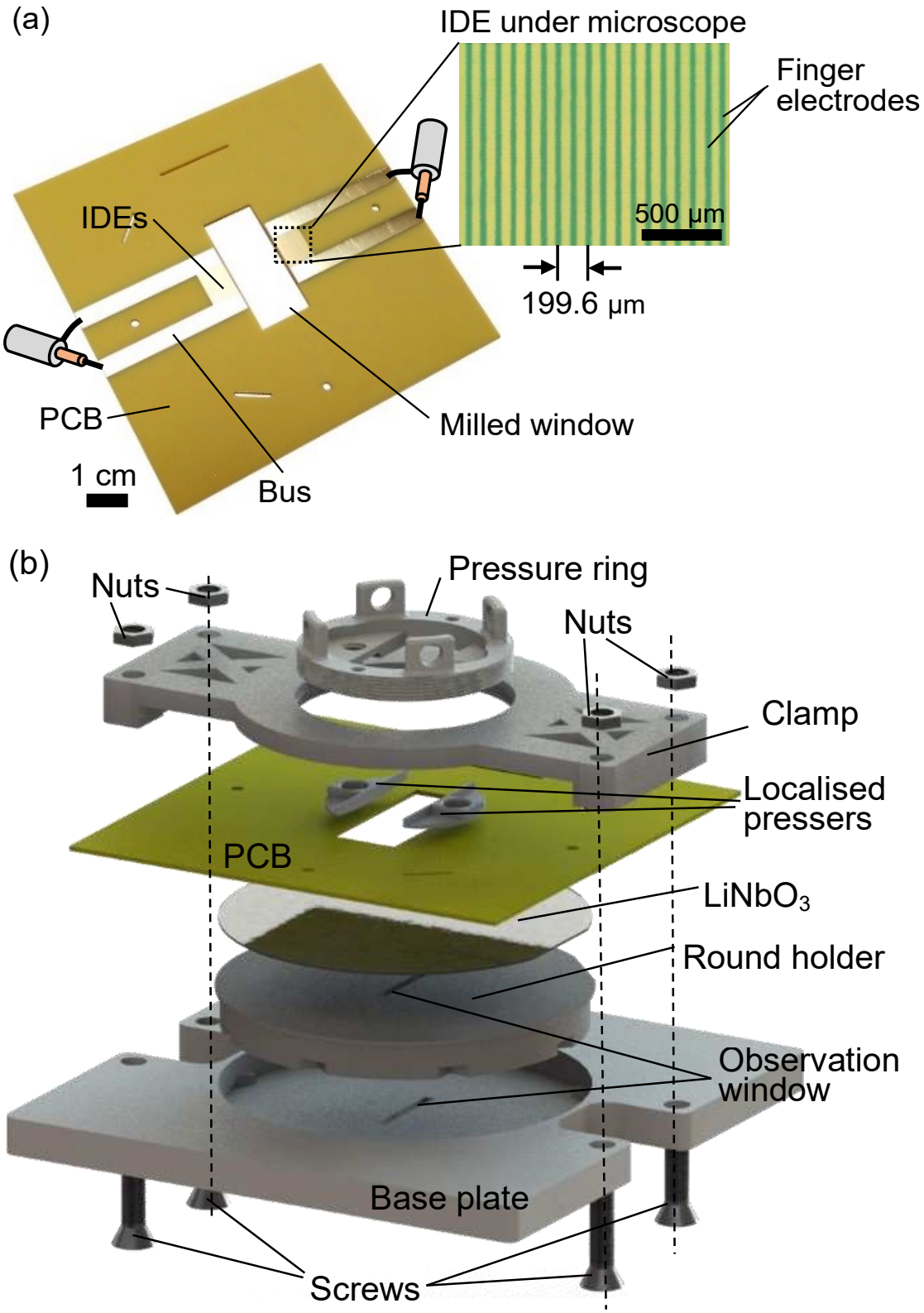
(a)
IDE under microscope
Finger electrodes
500 µm
199.6 µm
IDEs
PCB
1 cm
Bus
Milled window
(b)
Nuts
Pressure ring
Nuts
Clamp
Localised pressers
PCB
LiNbO3
Round holder
Observation window
Base plate
Screws

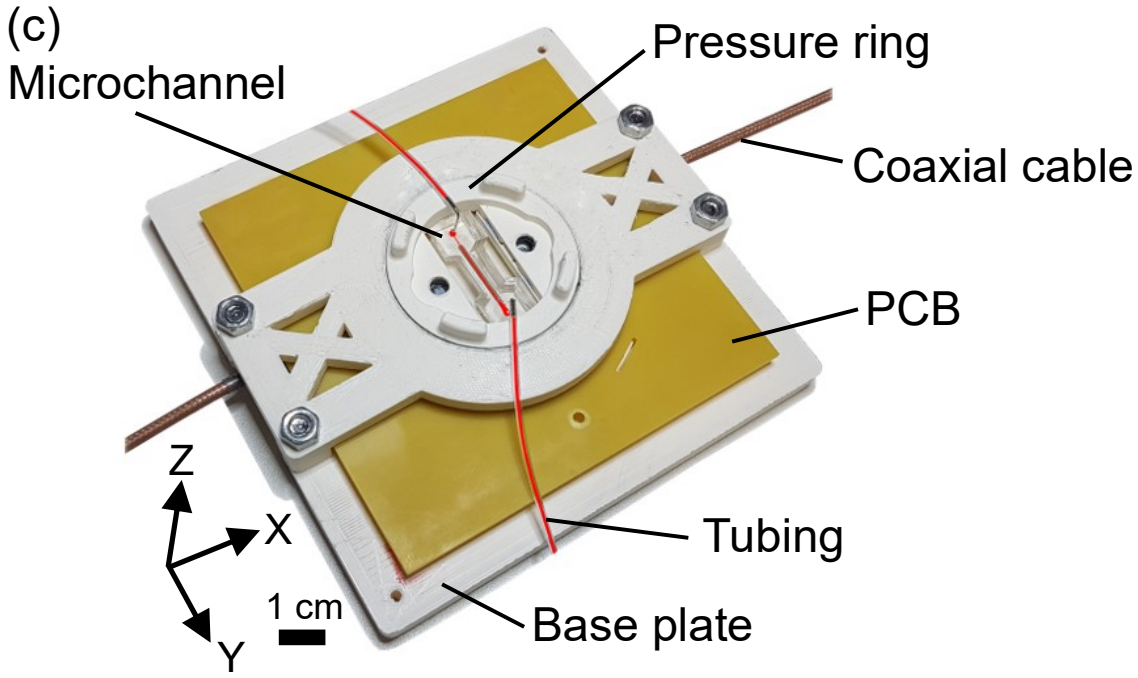

Figure 2. The components and assembly of the PCB-SAW device. (a) Pattern of the PCB and microscopic check of the IDEs on the PCB. (b) The assembly process of the PCB-SAW device. (c) The assembled PCB-SAW device.

(a)

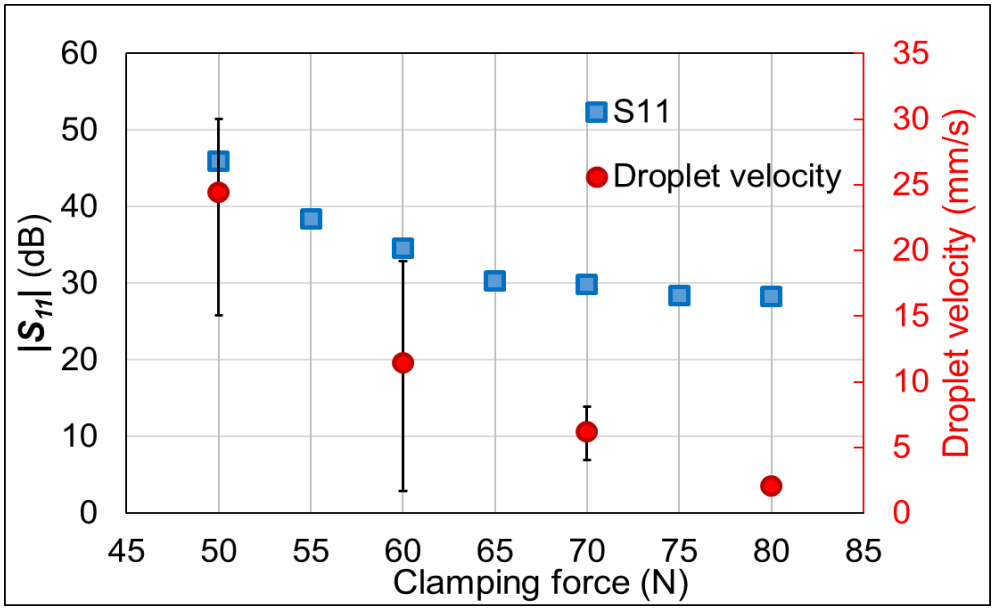
60
50
40
30
20
10
0
|S11| (dB)
35
30
25
20
15
10
5
0
Droplet velocity (mm/s)
S11
Droplet velocity
45
50
55
60
65
70
75
80
85
Clamping force (N)

(b)

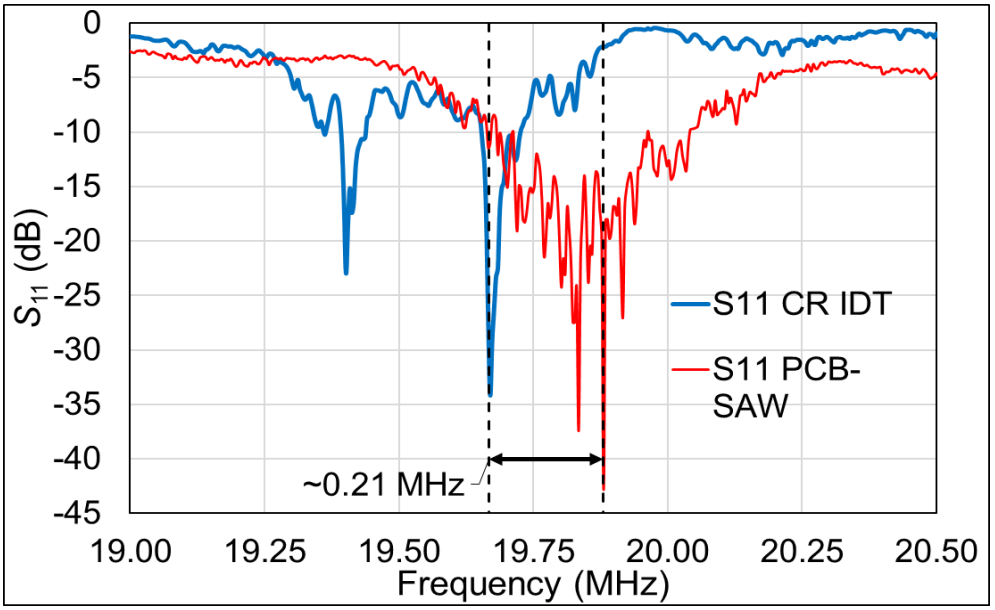
0
-5
-10
-15
-20
-25
-30
-35
-40
-45
S11 (dB)
S11 CR IDT
S11 PCB-SAW
~0.21 MHz
19.00
19.25
19.50
19.75
20.00
20.25
20.50
Frequency (MHz)

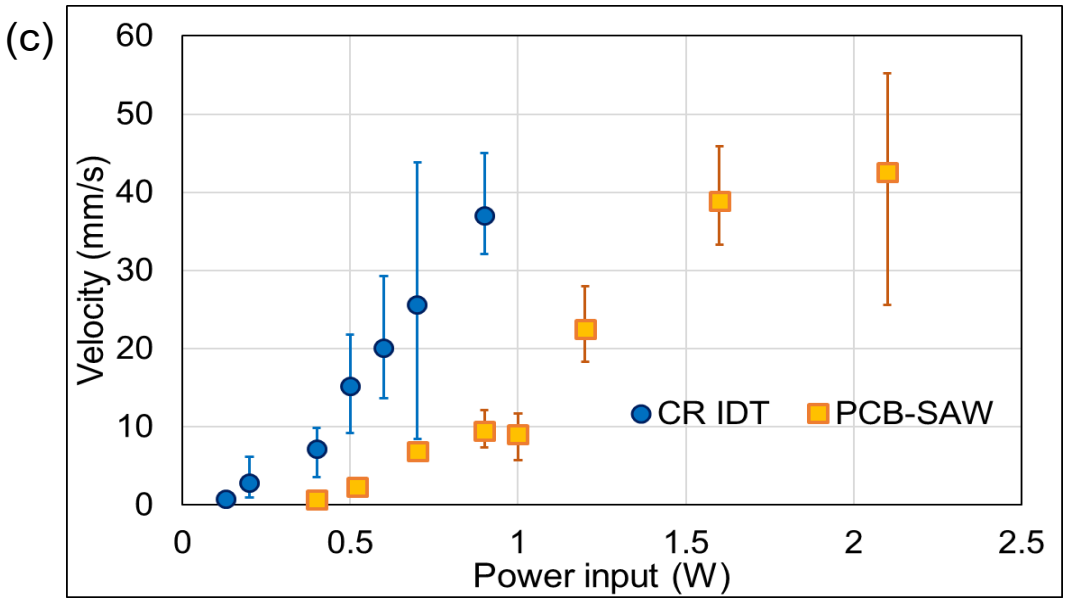

Figure 3. Characterisation of the PCB-SAW device and the comparations with the IDT made by photolithography in cleanroom (CR IDT). (a) The change of the S_{11} and the droplet velocity as the consequence of adding clamping force to the device. The droplet tests were done by applying an input power of 1.26 W. (b) Comparison between the S_{11} of the PCB-SAW device at 50 N and CR IDT, with the latter frequency being 19.67 MHz. (c) Comparation between the droplet velocities, which are driven by different input powers in the PCB-SAW device and CR IDT.

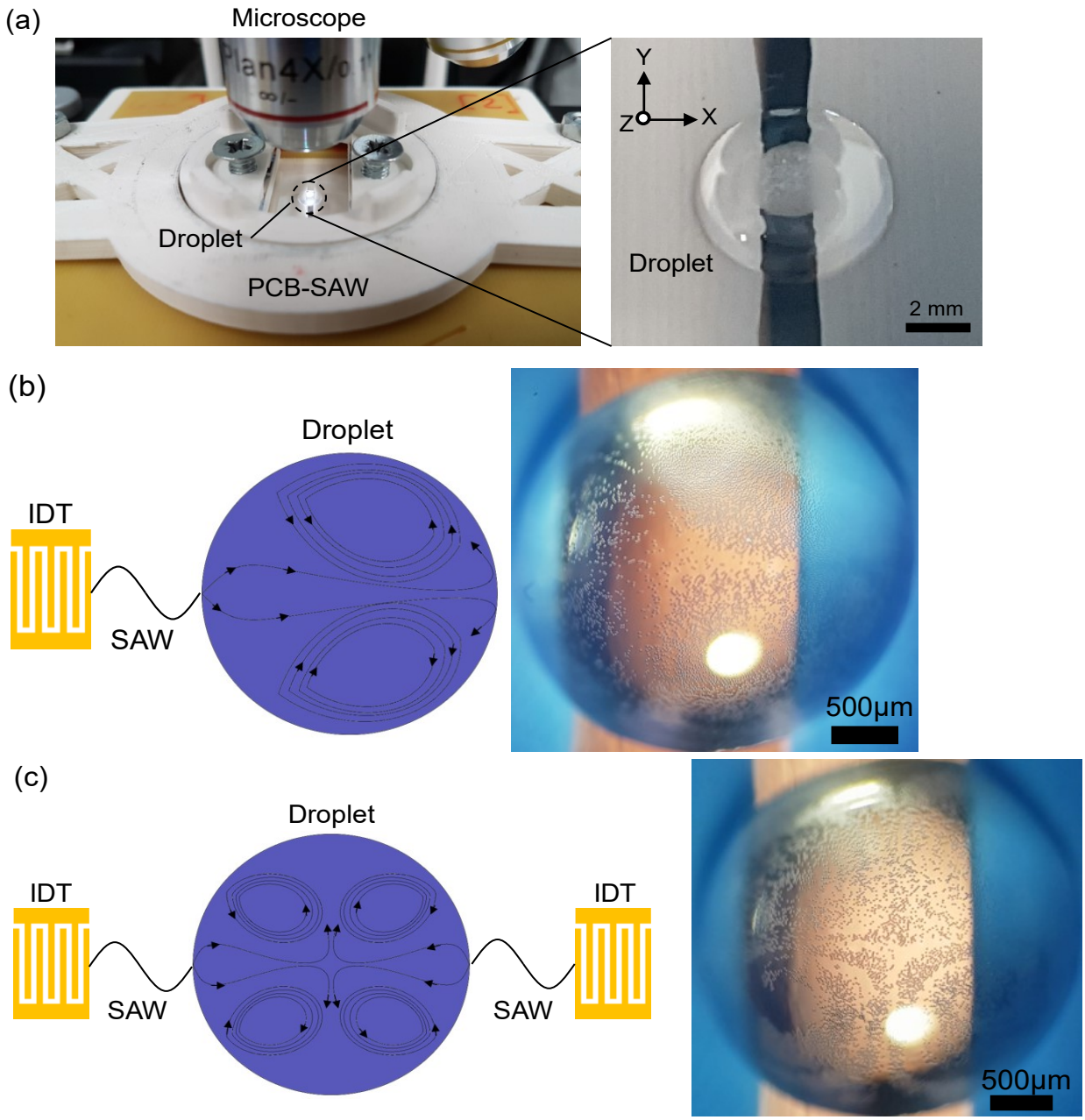

Figure 4. Testing the PCB-SAW device using droplet samples containing microspheres. (a) A droplet sample is applied to the PCB-SAW device at the centre of the two IDTs under a microscope. (b) A representation of the expected two-vortex streaming pattern and the experiment streaming pattern when one IDT is on (also in Video S1). (c) A representation of the expected four-vortex streaming pattern and the experiment streaming pattern when both IDTs are on (also in Video S2).

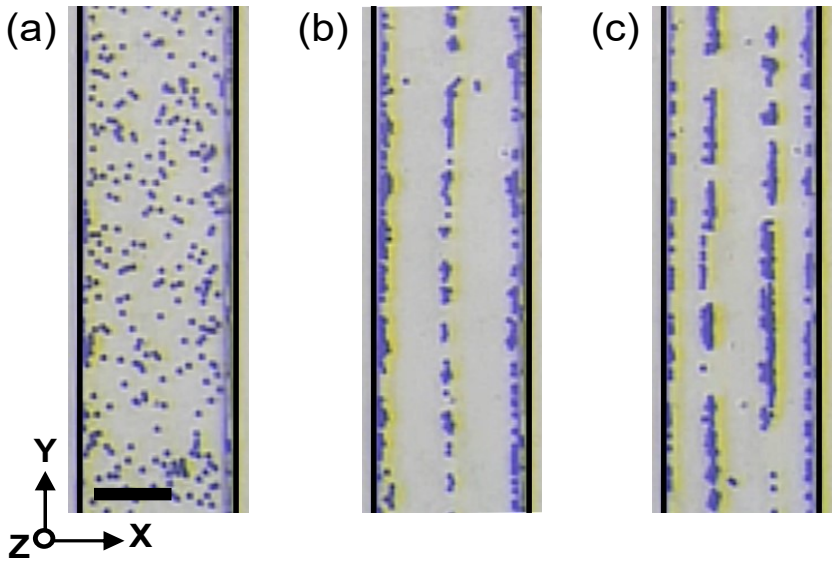

Figure 5. Particle trapping in the PCB-SAW device. (a) Microscopic image of 10 μm polystyrene microspheres evenly distributed inside the microchannel before applying SSAW. (b) Microscopic image of three microsphere traces inside the microchannel when applying SSAW with PNs located at the centre and near two sides of the microchannel. (c) Microscopic image of four microsphere traces inside the microchannel when applying SSAW with ANs located at the centre and near two sides of the microchannel. The scale bar is 100 μm.

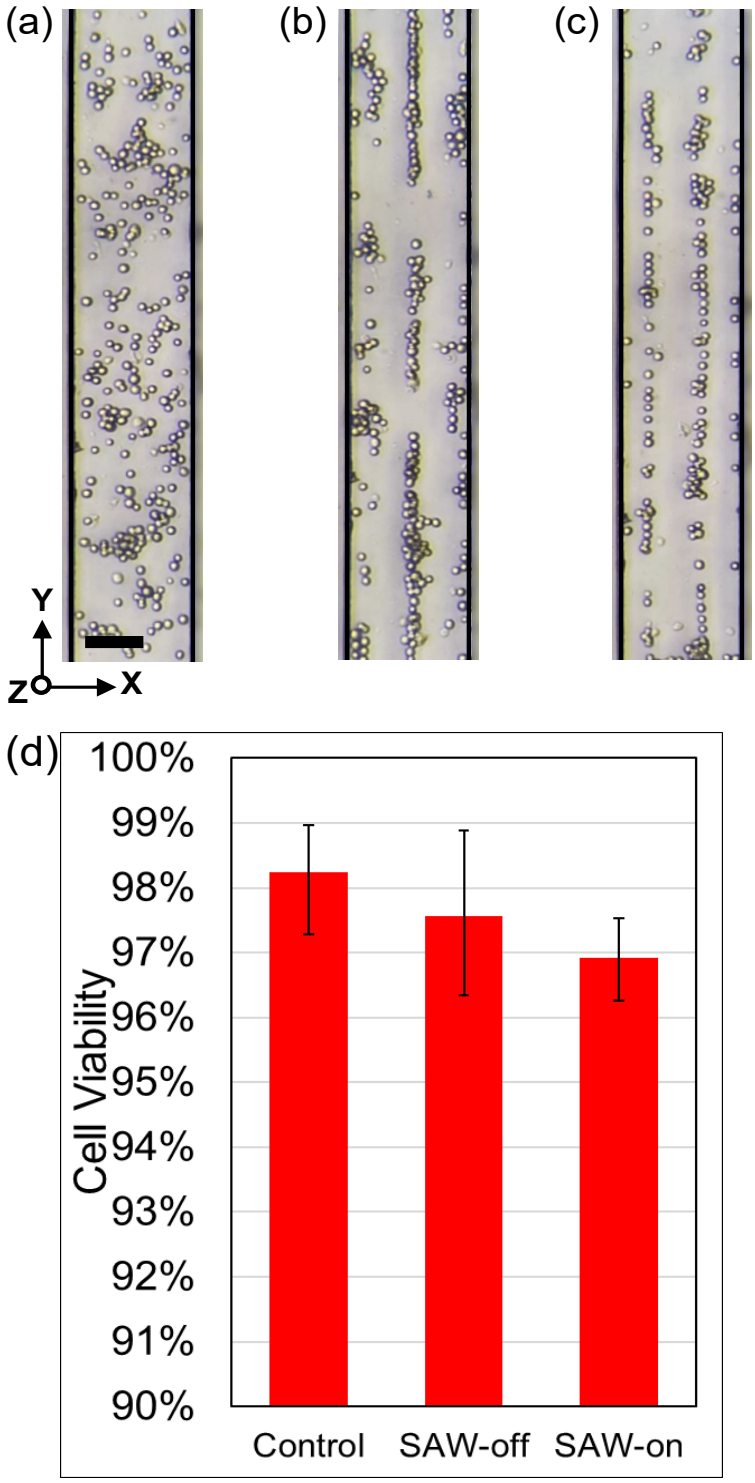

Figure 6. PCB-SAW manipulation of NSCLC cells. (a) Microscopic image of NSCLC cells evenly distributed inside the microchannel before applying SSAW. (b) Microscopic image of three cell traces inside the microchannel when applying SSAW with PNs located at the centre and near two sides of the microchannel. (c) Microscopic image of four cell traces inside the microchannel when applying SSAW with ANs located at the centre and near two sides of the microchannel. The scale bar is 100 μm. (d) Cell viability test for Control, SAW-off and SAW-on Groups, no significant viability change was found.